

# Synthesis and Characterization of graphene-oxide reinforced copper matrix composite

Isaque Moura, Talita Sousa, Andreza Lima, Wesley Oliveira and Luiz Brandão

Instituto Militar de Engenharia (IME),  
Rio de Janeiro, Brazil

2nd International Online-Conference on Nanomaterials  
IOCN

October 31, 2020



# Schedule

- 1 Introduction
  
- 2 Materials and Methods
  
- 3 Results and Discussion
  - Powders and GO morphology and microstructural analysis
  - Spectroscopy
  - Thermogravimetric Analysis (TGA)
  
- 4 Conclusions
  
- 5 Acknowledgments
  
- 6 References



# Introduction



# Introduction

The interest in the study and development of routes to increase copper resistance has received special attention from researchers in recent years.

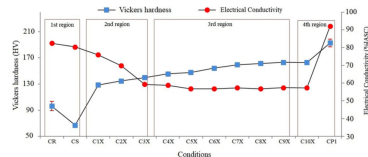


Figure: Evolution of the Vickers hardness and electrical conductivity of the CuCrZr alloy after ECAP treatment [1].

- Severe plastic deformation
- Cold rolling
- Composites

Such as:

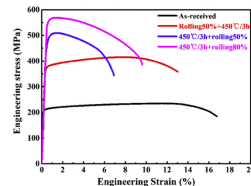


Figure: Stress-strain curves of the CuCrZr alloy with different treatment conditions [2].



# Introduction

## ■ Composites [3-5]

- 1 This method have been effective in improvement of copper mechanical properties, interfering less significantly in its electrical conductivity.
- 2 Carbon-based materials: Due to low solubility between copper and carbon, the diffusion of the carbonaceous material in the copper matrix is very low.
- 3 Utilization of Graphene.



# Introduction

## ■ Graphene and its derivatives [6-9]

- 1 Graphene is a planar carbon monolayer whose atoms are arranged in a two-dimensional form (2D).
- 2 Is considered the most resistant material ever tested (tensile strength values of 130 GPa).
- 3 High values of electrical ( $\sigma = 10^6 \Omega^{-1} cm^{-1}$ ) and thermal conductivity ( $5000 Wm^{-1} K^{-1}$ ).
- 4 Graphene oxide (GO) is the main derivative of graphene and its structure contains many oxygen-containing functional groups e.g. epoxy, hydroxyls, carbonyls and carboxyls linked to the layer of carbon atoms.



# Introduction

## ■ **Copper-Graphene composites** [10-12]

- 1 The manufacture of Cu-Gr composites has been studied through the use of several manufacturing techniques and different attempts to determine processing parameters.
- 2 The biggest challenges in Cu-Gr manufacture: the obtaining of an optimized dispersion of graphene in the matrix, favoring a good adhesion between the components and an attempt to minimize the agglomeration of graphene between grain boundaries.
- 3 The analysis of powders is essential due to the need to understand the changes that materials can undergo in their properties when performed different processes.



## Materials and Methods



# Preparation of Cu/GO composite

- The GO used in this study was produced by liquid-phase exfoliation (LPE), based on the method of Hummers and Offeman (1958) [13] and modified by Rourke et al. (2011) [14] and its final concentration was 4.55 mg/mL.
- Pure copper powder (Cu) with a purity of 99.94% was used as matrix.
- The preparation was followed as presented in flowchart bellow.



Figure: Flowchart of preparation Cu-Gr composite.



# Characterization

## SEM

- The morphologies of Copper and Cu/GO composite powders were observed by scanning electron microscopy (SEM).

## XRD

- X-Ray Diffraction was performed with Co  $K\alpha$  radiation and operated at 40 kV and 40 mA.

## Raman Spectra

- Raman spectra was performed on GO in order to observe the bands D and G, the wavelength of the laser used was 473 nm with a scanning range between 702 and 3343  $\text{cm}^{-1}$ , and an exposure time of 200s.



# Characterization

## TGA

- Thermogravimetric analysis was performed on GO and Cu/GO composites, and the samples were analyzed up to 800 °C in a controlled atmosphere of nitrogen, with a heating rate of 10 °C/min.

## FTIR

- Fourier transform infrared was performed on GO and Cu/GO composites and was taken with number of scans 60 and 4 cm<sup>-1</sup> resolution.



## Results and Discussion



# Powders and GO morphology and microstructural analysis

## ■ SEM

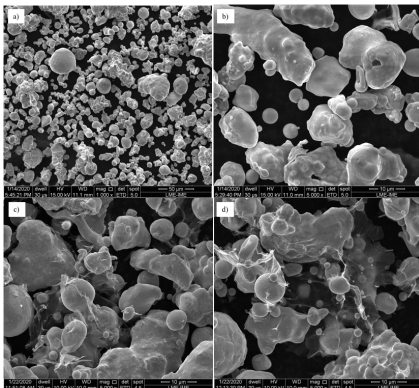


Figure: SEM (a,b) pure copper; (c,d) composite Cu/GO.

- Figure (a) and (b) the SEM images of the pure copper powder are presented.
- In Figure (c) and (d) the images of the copper-graphene composite are presented.
- It is possible to identify the GO sheets adhered to the surface of the copper particles and between the particles, showing adhesion between the copper and the GO.

# Powders and GO morphology and microstructural analysis

## ■ XRD

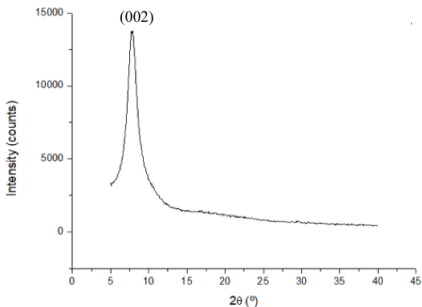


Figure: XRD of GO.

- The identified peak refers to the plane (002), indexed by the ICDD 03-065-6512 and is related to the HC structure of carbon. The diffraction peaks shown in the diffractogram refer to the leaves that are not arranged in the form of monolayers, as monolayers do not show a diffraction peak. Thus, there is an indication that the GO used for this study is formed by several layers



# Powders and GO morphology and microstructural analysis

## ■ XRD

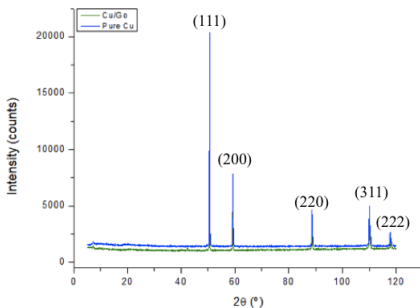


Figure: XRD of Pure copper and Cu/GO composite.

- The peaks referring to the FCC structure of copper and no other peak was indexed, ensuring that the copper powder did not have oxidation or other elements. Based on this result, it appears that there was no oxidation of copper in the mixture produced, or the present oxidation resulted in a very small amount of oxide, being insufficient to generate a peak above the noise of the diffractogram. In addition, no diffraction peak was observed for the GO, this is due to the concentration used to manufacture the composite being so low that it does not generate a diffraction peak.



# Raman Analysis

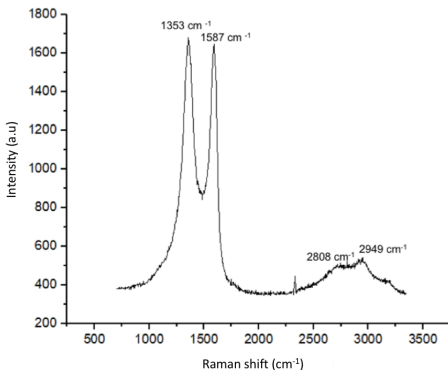


Figure: Raman spectra of GO used.

- The Raman Spectra of GO shows peaks referring to bands D ( $1353\text{ cm}^{-1}$ ) and G ( $1587\text{ cm}^{-1}$ ). The ratio of the intensities of bands D and G used in this study was approximately 1.0. In addition to the bands D and G, it was possible to observe the presence of the peaks referring to the bands 2D ( $2808\text{ cm}^{-1}$ ) and 2D' ( $2949\text{ cm}^{-1}$ ). These bands appear with less intensity in relation to the D and G bands and are related to the stacking of a number of carbon layers of the graphene structure [15]. Thus, the presence of these bands shows that the oxide analyzed is formed by stacking layers and not just monolayers, which can be confirmed by the XRD analysis.



# Fourier Transform Infrared Spectroscopy (FTIR)

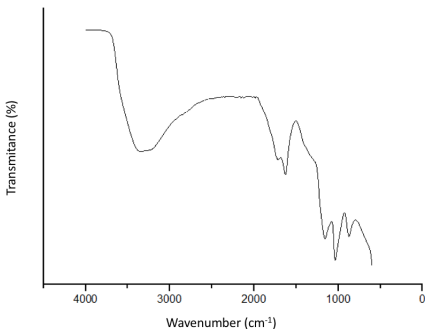


Figure: FTIR spectra of GO.

- The analysis of the spectrum allows us to initially observe the occurrence of a broad-band between  $3000$  to  $3700\text{ cm}^{-1}$ , which is related to the existence of water adsorbed between the leaves and a peak at  $3347\text{ cm}^{-1}$ , which can be attributed the OH stretching range. At  $1626\text{ cm}^{-1}$  a peak corresponding to the stretching vibrations of C=O is identified; followed by a third peak at  $1158\text{ cm}^{-1}$ , referring to vibrations of C-O-C epoxy groups;  $1036\text{ cm}^{-1}$ , vibrations of C-OH bonds and finally a last peak at  $873\text{ cm}^{-1}$ , due to the stretching vibrations of epoxy groups [16-18].



# Fourier Transform Infrared Spectroscopy (FTIR)

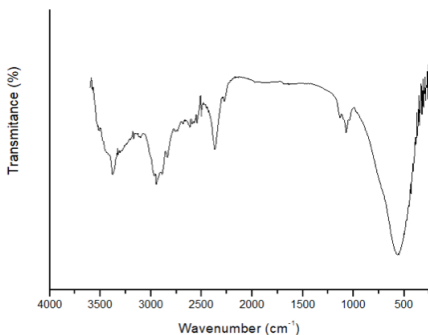


Figure: FTIR spectra of Cu/GO composite.

- For composite Cu/GO some characteristic peaks can be observed relative to the GO, such as the existence of a band present in approximately  $3500\text{ cm}^{-1}$ , related to the O-H elongation vibration. The absorption bands observed at  $2954\text{ cm}^{-1}$  can correspond to symmetric vibration of C-H bond [19]. At  $1060\text{ cm}^{-1}$ , a band related to C-O elongation (epoxy/ether) is noted. A peak appeared at  $596\text{ cm}^{-1}$ , which is attributed to observation of hydroxyl deformation modes [20-23].



# Thermogravimetric Analysis

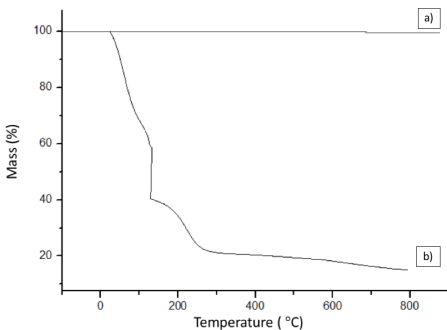


Figure: TGA of (a) Cu/GO composite and (b) GO.

- For the composite (a) it is notice that there is no change in mass as there was no gain its possible to deduce that there was no oxidation and the fact that there is no loss of weight is due to the low amount of graphene in the composite, being formed mainly of copper [24].
- For GO (b) it is observe a loss of mass below 100 °C, of 30%, associated with the elimination of adsorbed water and gas molecules. The range between 100-200 °C shows an abrupt loss of 34% in mass and between 200-300 °C of 13%, which are related to the elimination of functional groups. In the region of 300-600 °C the material remains stable, showing a small loss of mass, followed by a last loss in 600-800 °C, related to the removal of functional groups even more stable [16,17].



## Conclusions



# Conclusions

- Based on the results obtained by SEM and XRD, it is suggested that uniform mixtures of GO between the copper particles were obtained so that there were no large agglomerates.
- The mixing method through the mechanical stirring of the powder in aqueous dispersion was efficient to obtain the composite powder with good homogeneity and no oxidation.
- The GO used was formed by several layers, which was confirmed by the presence of 2D bands in Raman spectra.



## Acknowledgments



# Acknowledgments



UFRJ



Fundação de Amparo à Pesquisa do Estado do Rio de Janeiro



Conselho Nacional de Desenvolvimento Científico e Tecnológico



PUC  
RIO



## References



## References

- 1 SOUSA, T. G.; MOURA, I. A. B.; FILHO, F. C. G.; MONTEIRO, S. N.; BRANDAO, L. P. Combining severe plastic deformation and precipitation to enhance mechanical strength and electrical conductivity of Cu–0.65Cr–0.08Zr alloy. *Journal of Materials Research and Technology* 2020, 9, 5953–5961.
- 2 MENG, A.; NIE, J.; WEI, K. et al. Optimization of strength, ductility and electrical conductivity of a Cu–Cr–Zr alloy by cold rolling and aging treatment. *Vacuum* 2019, 167, 329–335.
- 3 ISHIDA, K.; NISHIZAWA, T. Alloy Phase Diagrams. In *ASM Handbook*; Eds. 10; ASM International, 1992.
- 4 SINGH, V.; JOUNG, D.; ZHAI, L.; DAS, S. KHONDAKER, S. I.; SEAL, S. Annealing induced electrical conduction and band gap variation in thermally reduced graphene oxide films with different sp<sup>2</sup>/sp<sup>3</sup> fraction. *Applied Surface Science*. 2015, 326, 236–242.
- 5 FADAVI, B, A. et al. Enhanced tensile properties of aluminium matrix composites reinforced with graphene encapsulated SiC nanoparticles. *Composites Part A: Applied Science and Manufacturing* 2015, 68, 155–163.
- 6 BALADIN, A. et al. Superior thermal conductivity of single-layer graphene. *Nano Lett.* 2008, 8, 902–907.
- 7 GEIM, A. K.; NOVOSELOV, K. S. The rise of graphene. *Nature Matter* 2007, 6, 183.
- 8 SAITO, K.; NAKAMURA, J.; NATORI, A. Ballistic thermal conductance of a graphene sheet *Phys. Rev. B.* 2007, 76.



## References

- 9 GAO, W.; ALEMANY, L. B.; CI, L.; AJAYAN, P. M. New insights into the structure and reduction of graphite oxide. *Nature Chemistry*. 2009, 1, 403–408.
- 10 AKTURK, A. and GOLDSMAN, N. Electron transport and full-band electron-phonon interactions in graphene. *Appl. Phys.* 2008, 103, 053702.
- 11 JAGANNADHAM, K. Thermal conductivity of copper-graphene composite films synthesized by eletrochemical deposition with exfoliated graphene platelets *Metallurgical and Materials Transactions*. 2011, 43, 316–324.
- 12 DUTKIEWICZ, J.; OZGA, P.; MAZIARZ, W. et al. Microstructure and properties of bulk copper matrix composites strengthened with various kinds of graphene nanoplatelets. *Materials Science Engineering A*. 2015, 628, 124–134.
- 13 HUMMERS, W. S.; OFFEMAN, R. E Preparation of Graphitic Oxide. 1957, 208, 1937–1957.
- 14 ROURKE, J. P.; et al. The Real Graphene Oxide Revealed: Stripping the Oxidative Debris from the Graphene-like Sheets. *Angew. Chem. Int.* 2011, 50, 3173–3177.
- 15 FERRARI, A. C.; BASKO, D. M. Raman spectroscopy as a versatile tool for studying the properties of graphene. *Nature nanotechnology* 2013, 8, 235–246.
- 16 PRUNA, A.; PULLINI, D.; BUSQUETS, D. Influence of synthesis conditions on properties of green-reduced graphene oxide. *Journal Nanopart Res.* 2013, 15, 1605.



## References

- 17 COROS, M. et al. Green synthesis, characterization and potential application of reduced graphene oxide. *Physica E: Low-dimensional Systems and Nanostructures*. 2020, 119, 113971.
- 18 GHADIM et al. Pulsed laser irradiation for environment friendly reduction of graphene oxide suspensions *Applied Surface Science* 2014, 301, 183–188.
- 19 CHANDRA, A.; SINGH, A. Graphite oxide/polypyrrole composite electrodes for achieving high energy density supercapacitors. *J. Appl. Electrochem.* 2013, 43, 773–782.
- 20 HWANG, J.; YOON, T., JIN, S. H. et al. Enhanced mechanical properties of graphene/copper nanocomposites using a molecular-level mixing process. *Adv. Mater* 2013, 25, 6724–6729.
- 21 ROUESSAC, F.; ROUESSAC, A.; BROOKS, S. *Chemical Analysis Modern Instrumentation Methods and Techniques*. In John Wiley and Sons Ltd; Eds. 2; 2007, 1992.
- 22 LORYUENYONG, V.; et al. Preparation and characterization of reduced graphene oxide sheets via water-based exfoliation and reduction methods. *Ann. Mater. Sci. Eng.* 2013, 352, 403–411.
- 23 SARKAR, C.; DOLUI, S. K. Synthesis of copper oxide/reduced graphene oxide nanocomposite and its enhanced catalytic activity towards reduction of 4- nitrophenol *RSC Adv.* 2015, 5, 60–72.
- 24 ZHANG, L. et al. In situ synthesis of three-dimensional graphene skeleton copper azide with tunable sensitivity performance. *Materials Letters*. 2020, 279, 128466.

